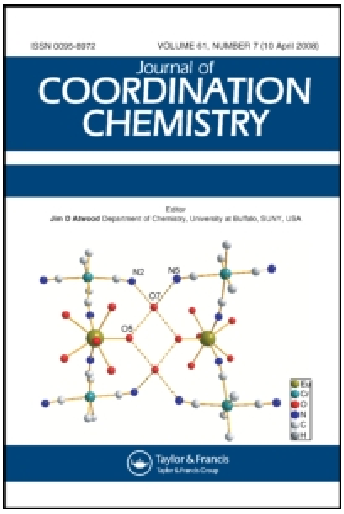

Journal of Coordination Chemistry
Publication details, including instructions for authors and subscription information:
http://www.informaworld.com/smpp/title~content=t713455674

Synthesis, spectral, magnetic, electrochemical and catalytic studies of cyclam-based copper(II) and nickel(II) complexes-effect of N-substitution

S. Sreedaran[a]; K. Shanmuga Bharathi[a]; A. Kalilur Rahiman[a]; K. Rajesh[a]; G. Nirmala[a]; V. Narayanan[a]
[a] Department of Inorganic Chemistry, University of Madras, Chennai, Tamil Nadu-600 025, India

To cite this Article Sreedaran, S. , Shanmuga Bharathi, K. , Kalilur Rahiman, A. , Rajesh, K. , Nirmala, G. and Narayanan, V.(2008) 'Synthesis, spectral, magnetic, electrochemical and catalytic studies of cyclam-based copper(II) and nickel(II) complexes-effect of N-substitution', Journal of Coordination Chemistry, 61: 22, 3594 — 3609

To link to this Article: DOI: 10.1080/00958970802087425

URL: http://dx.doi.org/10.1080/00958970802087425

Journal of Coordination Chemistry
Vol. 61, No. 22, 20 November 2008, 3594–3609

Synthesis, spectral, magnetic, electrochemical and catalytic studies of cyclam-based copper(II) and nickel(II) complexes – effect of N-substitution

S. SREEDARAN, K. SHANMUGA BHARATHI, A. KALILUR RAHIMAN, K. RAJESH, G. NIRMALA and V. NARAYANAN*

Department of Inorganic Chemistry, University of Madras, Guindy Campus, Chennai, Tamil Nadu–600 025, India

(*Received 18 August 2007; in final form 30 January 2008*)

New *N*-substituted cyclam ligands 1,8-[*bis*(3-formyl-2-hydroxy-5-methyl)benzyl]-1,4,8,11-tetraazacyclotetradecane, 1,8-[*bis*(3-formyl-2-hydroxy-5-methyl)benzyl]-4,11-dimethyl-1,4,8,11-tetraazacyclotetradecane, 1,8-[*bis*(3-formyl-2-hydroxy-5-bromo)benzyl]-1,4,8,11-tetraazacyclo tetradecane, and 1,8-[*bis*(3-formyl-2-hydroxy-5-bromo)benzyl]-4,11-dimethyl-1,4,8,11-tetraazacyclotetradecane (L^1–L^4) were synthesized and mononuclear copper(II) and nickel(II) complexes prepared. The ligands and complexes were characterized by elemental analysis, electronic, IR, ^{1}H NMR and ^{13}C NMR spectral studies. *N*-alkylation causes red shifts in the λ_{max} values of the complexes. Copper(II) complexes show one-electron, quasi-reversible reduction waves in the range -1.04 to -1.00 V. The nickel(II) complexes show one-electron, quasi-reversible reduction waves in the range -1.18 to -1.30 V and one-electron, quasi-reversible oxidation waves in the range $+1.20$ to $+1.40$ V. The reduction potential of the copper(II) and nickel(II) complexes of the ligands L^1 to L^2 and L^3 to L^4 shift anodically on N-alkylation. The ESR spectra of the mononuclear copper(II) complexes show four lines, characteristic of square-planar geometry with nuclear hyperfine spin 3/2. All copper(II) complexes show a normal room temperature magnetic moment value $\mu_{eff} = 1.70$–1.74 BM which is close to the spin only value of 1.73 BM. Kinetic studies on the oxidation of pyrocatechol to o-quinone using the copper(II) complexes as catalysts and on the hydrolysis of 4-nitrophenylphosphate using the copper(II) and nickel(II) complexes as catalyst were carried out. The tetra-N-substituted complexes have higher rate constants than the corresponding disubstituted complexes.

Keywords: Cyclam; Nickel complexes; Copper complexes; Catecholase activity; Hydrolysis of nitrophenyl phosphate

1. Introduction

The synthesis of 1,4,8,11-tetraazacyclotetradecane (cyclam) and substituted cyclam ligands to control and tune coordination properties of transition and lanthanide metal complexes has been the subject of growing interest [1–3]. Among the range of

---

*Corresponding author. Email: vnnara@yahoo.co.in

Journal of Coordination Chemistry
ISSN 0095-8972 print/ISSN 1029-0389 online © 2008 Taylor & Francis
DOI: 10.1080/00958970802087425

tetraazamacrocyclic ligands, cyclam and cyclen are the two most important tetraazamacrocycles and their complexes have been widely used as MRI contrasting agents [4], luminescent probes [5], DNA cleavers [6], and medicines for radiopharmaceutical applications [7]. Tetraazamacrocyclic ligands bearing additional pendant coordination side arms have been of particular interest, as their properties and selectivity for certain metal ions may be quite different from those of the unsubstituted parent macrocycles [8–10]. Understanding of N-substitution of the ligand on coordination remains an important field of research. Copper catalyzed oxidation of phenols [11, 12] and hydrolysis of the active sites in a number of enzymes by nickel ions [13] are important chemical processes in biological systems. Herein, we report the synthesis of a series of new N-substituted cyclam ligands (L^1–L^4) containing a highly reactive free aromatic formyl group and phenolic oxygen as additional co-coordinating groups. Mononuclear copper(II) and nickel(II) complexes of these ligands are also reported The formyl group can be condensed with a fluorescent moiety [14], or redox active molecules, to be used for sensor applications [15] in the future. The cavity size and the shape of the molecule can be easily tuned to study the coordination properties of the ligands. Effect of N-substitution on the spectral, electrochemical, and catalytic properties of these complexes are also discussed.

2. Experimental

2.1. *Chemicals and reagents*

1,4,8,11-Tetraazacyclotetradecane (cyclam) [16], 5-methyl salicylaldehyde [17], 3-chloromethyl-5-methyl salicylaldehyde, 3-chloromethyl-5-bromo salicylaldehyde [18] and 1,4,8,11-tetraazatricyclo[9.3.1.1^{4,8}]hexadecane [19] were prepared by literature methods. Analytical grade methanol, acetonitrile and dimethylformamide were purchased from Qualigens and used as received. TBAP (tetrabutylammonium perchlorate) used as supporting electrolyte in electrochemical measurement was purchased from Fluka and recrystallized from hot methanol. (**Caution!** TBAP is potentially explosive; hence care should be taken in handling the compound.) All other chemicals and solvents were analytical grade and were used as received.

2.2. *Analytical and physical measurements*

Elemental analysis of the complexes was obtained using a Haereus CHN rapid analyzer and ^{1}H NMR spectra were recorded using a JEOL GSX 400 MHZ NMR spectrometer. Electronic spectral studies were carried out on a Hitachi 320 spectrophotometer in the range 200–800 nm. IR spectra were recorded on a Shimadzu FTIR 8300 series spectrophotometer on KBr disks in the range 4000 to 400 cm^{-1}. Molar conductivity was measured by using an Elico digital conductivity bridge model CM-88 using freshly prepared solution of the complex in dimethylformamide. Cyclic voltammograms were obtained on a CHI-600A electrochemical analyzer. The measurements were carried out under oxygen-free conditions using a three-electrode cell in which a glassy carbon electrode was the working electrode, a saturated Ag/AgCl electrode was the reference electrode and platinum wire was used as the auxiliary electrode. A ferrocene/ferrocenium (1+) couple was used as an internal standard and $E_{1/2}$ of the ferrocene/ferrocenium (Fc/Fc^+) couple under the experimental condition is 470 mV. Tetra(n-butyl)ammonium perchlorate (TBAP) was used as the supporting electrolyte. Room temperature magnetic moments were measured on a PAR vibrating sample magnetometer Model-155. X-band ESR spectra were recorded at 25°C on a Varian EPR-E 112 spectrometer using diphenylpicrylhydrazine (DPPH) as the reference. The atomic absorption spectral data were recorded using a Varian spectra AA-200 model atomic absorption spectrophotometer. Mass spectra were obtained on a JEOL SX-102 (FAB) mass spectrometer. Catalytic oxidation of catechol to o-quinone by the copper complexes and hydrolysis of 4-nitrophenylphosphate by the copper and nickel complexes were studied in 10^{-3} M dimethylformamide solutions. The reactions were followed spectrophotometrically with the strongest absorption band of o-quinone at 390 nm and monitoring the increase in absorbance; the hydrolysis of p-nitrophenylphosphate was monitored by following the UV absorbance change at 420 nm (assigned to the 4-nitrophenolate anion) as a function of time. A plot of $\log (A\alpha/A\alpha - A_t)$ *versus* time was made for each complex and the rate constants for the catalytic oxidations and the hydrolyses of 4-nitrophenylphosphate were calculated.

2.3. *Synthesis of precursor compound (PC-1)*

The compound 1,4,8,11-tetraazatricyclo[9.3.1.1^{4,8}]hexadecane (0.29 g, 0.0013 mol) was dissolved in acetonitrile (30 mL) and two equivalents of 3-chloromethyl-5-methyl salicylaldehyde (0.48 g, 0.0026 mol) in acetonitrile (30 mL) was rapidly added. This solution was stirred at room temperature (25°C) for 24 h and the yellow precipitate which formed was filtered, washed with a small quantity of acetonitrile and dried under vacuum. This crude compound 1,8-[*bis*(3-formyl-2-hydroxy-5-methyl)benzyl]-4,11-diazaniatricyclo[9.3.1.1^{4,8}]-hexadecane dichloride was recrystallized from water to give white crystals. Yield-90%. M.p-278°C. IR (KBr): 3393 cm^{-1}, 1680 cm^{-1}; ^1H NMR: δ (ppm in DMSO-D_6), 1.23 (q, 4H, β-CH_2), 2.57 (m, 16H, α-CH_2), 3.24 (s, 4H, N–CH_2–N) 4.10 (s, 4H, N–CH_2–Ar), 7.34 (d, 4H, Ar–H), 9.86 (s, 2H, Ar–CHO). ^{13}C NMR: δ (ppm in DMSO-D_6), 28.3, 49.1, 54.4, 55.2, 55.8, 56.2, 60.5, 78.6, 122.1, 124.8, 126.2, 131.0, 136.1, 159.6, 196.6.

2.4. *Synthesis of L^1*

PC-1 (1 g, 0.0017 mol) was dissolved in 200 mL of aqueous NaOH (0.3 M) with stirring. After stirring for 4 h, the solution was extracted with $CHCl_3$ (5 × 30 mL). The combined $CHCl_3$ extracts were dried with anhydrous $MgSO_4$ and concentrated under vacuum to give 1,8-[*bis*(3-formyl-2-hydroxy-5-methyl)benzyl]-1,4,8,11-tetraazacyclotetradecane. Yield: 72%. M.p.: 282°C (dec). Anal. Calcd for $C_{28}H_{40}N_4O_4$ (%): C, 67.72; H, 8.12; N, 11.28. Found: C, 67.64; H, 8.02; N, 11.17. IR data (KBr disc): 3389 cm^{-1}, 3285 cm^{-1}, 1680 cm^{-1}. ^1H NMR: δ (ppm in $CDCl_3$), 1.54 (q, 4H, β-CH_2), 2.32 (m, 16H, α-CH_2), 2.56 (br, s, 2H, NH), 4.1 (s, 4H, N–CH_2–Ar), 7.26 (d, 4H, Ar–H), 9.92 (s, 2H, Ar–CHO), 12.54 (br, s, Ar–OH). ^{13}C NMR: δ (ppm in DMSO-D_6), 28.3, 49.4, 54.8, 55.2, 55.7, 60.5, 122.4, 126.2, 126.8, 131.0, 136.8, 157.6, 196.0.

2.5. *Synthesis of* L^2

PC-1 (1 g, 0.0017 mol) was dissolved in EtOH/H_2O (95 : 5 v/v) mixture. 10 equivalents of $NaBH_4$ were then added and the mixture was refluxed for 3 h. After cooling to room temperature, 10 mL of HCl (3 M in water) was added. The mixture was concentrated to dryness and the residue was then dissolved in 100 mL of water and concentrated KOH was added (pH = 12). After extraction with $CHCl_3$ (5 × 30 mL) the organic phase was collected, dried with anhydrous $MgSO_4$ and concentrated to give 1,8-[*bis*(3-formyl-2-hydroxy-5-methyl)benzyl]-4,11-dimethyl-1,4,8,11-tetraazacyclotetradecane. Yield: 84%. M.p.: 280°C (dec). Anal. Calcd for $C_{30}H_{38}N_4O_4$ (%): C, 69.47; H, 7.38; N, 10.80. Found: C, 69.38; H, 7.27; N, 10.72. IR (KBr): 3365 cm^{-1}, 1676 (s) cm^{-1}. ^1H NMR (ppm in $CDCl_3$): δ 1.54 (q, 4H, β-CH_2), 2.32 (t, 16H, α-CH_2), 2.65 (br, s, 6H, N–CH_3), 4.1 (s, 4H, N–CH_2–Ar), 7.32 (d, 4H, Ar–H), 9.98 (s, 2H, Ar–CHO), 12.32 (br, s, Ar–OH). ^{13}C NMR: δ (ppm in DMSO-D_6), 30.1, 49.7, 54.7, 55.0, 55.8, 60.2, 124.1, 124.8, 126.5, 133.0, 136.4, 157.6, 196.0.

2.6. *Synthesis of precursor compound (PC-2)*

The compound 1,8-[*bis*(3-formyl-2-hydroxy-5-bromo)benzyl]-4,11-diazaniatricyclo[9.3.1.1^{4,8}]hexadecane dichloride (PC-2) was prepared by following the procedure of PC-1 using two equivalents of 3-chloromethyl-5-bromo salicylaldehyde (0.0026 mol, 0.65 g), instead of 3-chloromethyl-5-methyl salicylaldehyde. Yield: 90%, M.p.: 282°C, IR (KBr): 3405 cm^{-1}, 1680 cm^{-1}. ^1H NMR (δ ppm in DMSO-D_6), 1.23 (q, 4H, β-CH_2), 2.12 (t, 16H, α-CH_2), 4.1 (s, 4H, N–CH_2–Ar), 7.74 (d, 4H, Ar–H), 10.22 (s, 2H, Ar–CHO). ^{13}C NMR: δ (ppm in DMSO-D_6), 28.0, 49.4, 54.5, 54.8, 55.2, 55.7, 61.2, 78.2, 123.1, 125.3, 126.2, 130.0, 136.1, 158.6, 196.4.

2.7. *Synthesis of* L^3

1,8-[*bis*(3-formyl-2-hydroxy-5-bromo)benzyl]-1,4,8,11-tetraazacyclotetradecane was prepared by using (PC-2) (1 g, 0.0014 mol) instead of PC-1. Yield: 75%. M.p.: 300°C (dec). Anal. Calcd for $C_{26}H_{34}N_4O_4Br_2$ (%): C, 49.86; H, 5.47; N, 8.95. Found: C, 49.78; H, 5.42; N, 8.87. IR (KBr): 3407 cm^{-1}, 3289 cm^{-1}, 1680 cm^{-1}. ^1H NMR: δ (ppm in $CDCl_3$), 1.49 (q, 4H, β-CH_2), 2.56 (br, s, 2H, NH), 2.38 (m, 16H, α-CH_2), 3.39 (s, 4H, N–CH_2–N), 4.1 (s, 4H, N–CH_2–Ar), 7.76 (d, 4H, Ar–H), 10.20 (s, 2H, Ar–CHO), 12.64 (br, s, Ar–OH). ^{13}C NMR: δ(ppm in DMSO-D_6), 29.8, 49.7, 53.7, 55.0, 55.6, 61.6 122.6, 124.8, 126.0, 131.0, 136.1, 159.0, 196.0.

2.8. *Synthesis of* L^4

1,8-[*bis*(3-formyl-2-hydroxy-5-bromo)benzyl]-4,11-dimethyl-1,4,8,11-tetraazacyclotetradecane was prepared by using (PC-2) (1 g, 0.0014 mol) instead of PC-1. Yield: 70%. M.p.: 285°C (dec). Anal. Calcd for $C_{28}H_{38}N_4O_4Br_2$ (%): C, 51.39; H, 5.85; N, 8.56. Found: C, 51.34; H, 5.78; N, 8.49. IR (KBr): 3409 cm^{-1}, 3278 cm^{-1}, 1676 cm^{-1}. ^1H NMR (ppm in $CDCl_3$): δ 1.62 (q, 4H, β-CH_2), 2.32 (t, 16H, α-CH_2), 2.37 (s, 6H, N–CH_3), 4.1 (s, 4H, N–CH_2–Ar), 7.32 (d, 4H, Ar–H), 10.24 (s, 2H, Ar–CHO), 12.32 (s, cAr–OH). ^{13}C NMR: δ (ppm in DMSO-D$_6$), 33.4, 50.7, 54.0, 54.4, 55.2, 62.2, 122.0, 124.8, 126.3, 132.1, 136.7, 157.9, 196.2.

2.9. *Synthesis of macrocyclic mononuclear complexes*

The copper(II) and nickel(II) complexes were prepared by refluxing the respective metal perchlorate hexahydrate (1 mmol) in methanol (50 mL) with appropriate ligand (1 mmol) in methanol (50 mL). The resulting solution was refluxed for 8 h, filtered while hot and allowed to stand at room temperature. After evaporation of the solvent, the compound was recrystallized from acetonitrile to get pure complex.

2.9.1. [CuL^1](ClO$_4$)$_2$. Dark brown solid. Yield: 75%. Anal. Calcd for [$C_{28}H_{40}N_4O_4Cu$](ClO_4)$_2$: C, 44.30; H, 5.31; N, 7.38; Cu, 8.37. Found: C, 44.38; H, 5.10; N, 7.31; Cu, 8.41 (%). FAB mass [M–ClO$_4$]$^+$: 660. Conductance (Λ_m/S cm^2 mol^{-1}) in CH$_3$CN: 139.

2.9.2. [CuL^2](ClO$_4$)$_2$. Dark brown solid. Yield: 72%. Anal. Calcd for [$C_{30}H_{44}N_4O_4Cu$](ClO_4)$_2$: C, 45.78; H, 5.63; N, 7.12; Cu, 8.07. Found: C, 45.69; H, 5.57; N, 7.09; Cu, 7.97%. FAB mass [M–ClO$_4$]$^+$: 688. Conductance (Λ_m/S cm^2 mol^{-1}) in CH$_3$CN: 152.

2.9.3. [NiL^1](ClO$_4$)$_2$. Yellowish green compound. Yield: 72%. Anal. Calcd for [$C_{28}H_{40}N_4O_4Ni$](ClO_4)$_2$: C, 44.59; H, 5.34; N, 7.43; Ni, 7.78. Found: C, 44.63; H, 5.32; N, 7.37; Ni, 7.71%. ^{1}H NMR (ppm in CDCl$_3$): δ 1.71–1.76 (q, 4H, β-CH$_2$), 2.27 (s, 6H, Ar–CH$_3$), 2.39–2.60 (m, α-CH$_2$), 3.2 (s, 2H, NH), 3.56 (s, 4H, N–CH$_2$–Ar), 7.0–7.12 (d, 4H, Ar–H), 10.34 (s, 2H, Ar–CHO), 13.82 (s, Ar–OH). FAB mass [M–ClO$_4$]$^+$: 655. Conductance (Λ_m/S cm^2 mol^{-1}) in CH$_3$CN: 133.

2.9.4. [NiL^2](ClO$_4$)$_2$. Yellowish green compound. Yield: 70%. Anal. Calcd for [$C_{30}H_{44}N_4O_4Ni$](ClO_4)$_2$: C, 46.06; H, 5.67; N, 7.16; Ni, 7.50. Found: C, 46.02; H, 5.58; N, 7.31; Ni, 7.11%. ^{1}H NMR (ppm in CDCl$_3$): δ 1.74–1.82 (q, 4H, β-CH$_2$), 2.28 (s, 6H, Ar–CH$_3$), 2.43–2.60 (m, 8H, α-CH$_2$), 3.2 (s, 2H, NH), 3.39–3.43 (m, 8H, –N–CH$_2$), 3.56 (s, 4H, N–CH$_2$–Ar), 7.0–7.12 (d, 4H, Ar–H), 10.34 (s, 2H, Ar–CHO), 13.80 (s, Ar–OH). FAB mass [M–ClO$_4$]$^+$: 687. Conductance (Λ_m/S cm^2 mol^{-1}) in CH$_3$CN: 149.

2.9.5. [CuL^3](ClO$_4$)$_2$. Dark brown solid. Yield: 74%. Anal. Calcd for [$C_{26}H_{34}N_4O_4Br_2Cu$](ClO_4)$_2$: C, 35.13; H, 3.86; N, 6.30; Cu, 7.15. Found: C, 35.16; H, 3.69; N, 6.30; Cu, 7.10%. FAB mass [M–2ClO$_4$]$^+$: 689. Conductance (Λ_m/S cm^2 mol^{-1}) in CH$_3$CN: 157.

2.9.6. [CuL^4](ClO$_4$)$_2$. Dark brown solid. Yield: 71%. Anal. Calcd for [$C_{28}H_{38}N_4O_4Br_2Cu$](ClO_4)$_2$: C, 36.68; H, 4.18; N, 6.11; Cu, 6.93. Found: C, 36.66;

H, 4.09; N, 6.09; Cu, 6.84%. FAB mass $[M–2ClO_4]^+$: 718. Conductance (Λ_m/S cm^2 mol^{-1}) in CH_3CN: 159.

2.9.7. $[NiL^3](ClO_4)_2$. Yellowish green compound. Yield: 75%. Anal. Calcd for $C_{26}H_{34}N_4O_4Br_2Ni](ClO_4)_2$: C, 35.33; H, 3.88; N, 6.34; Ni, 6.64. Found: C, 35.36; H, 3.57; N, 6.30; Ni, 6.58%. ^{1}H NMR (ppm in $CDCl_3$): δ 1.69–1.82 (q, 4H, β-CH_2), 2.28 (s, 6H, Ar–CH_3), 2.40–2.64 (m, 8H, NH–CH_2), 3.21 (s, 2H, NH), 3.41–3.45 (m, 8H, N–CH_2), 3.56 (s, 4H, N–CH_2–Ar), 7.21–7.30 (d, 4H, Ar–H), 10.34 (s, 2H, Ar–CHO), 13.82 (s, Ar–OH). FAB mass $[M–ClO_4]^+$: 784. Conductance (Λ_m/S cm^2 mol^{-1}) in CH_3CN: 143.

2.9.8. $[NiL^4](ClO_4)_2$. Yellowish green compound. Yield: 75%. Anal. Calcd for $[C_{28}H_{38}N_4O_4Br_2Ni](ClO_4)_2$: C, 36.87; H, 4.20; N, 6.14; Ni, 6.44. Found: C, 36.77; H, 4.11; N, 6.13; Ni, 6.33%. ^{1}H NMR (ppm in $CDCl_3$): δ 1.69–1.82 (q, 4H, β-CH_2), 2.28 (s, 6H, Ar–CH_3), 2.40–2.64 (m, 16H, α-CH_2), 3.20 (s, 2H, NH), 3.58 (s, 4H, N–CH_2–Ar), 7.21–7.32 (d, 4H, Ar–H), 10.34 (s, 2H, Ar–CHO), 13.78 (s, Ar–OH). FAB mass $[M–ClO_4]^+$: 813. Conductance (Λ_m/S cm^2 mol^{-1}) in CH_3CN: 147.

3. Results and discussion

The precursor compounds PC-1 and PC-2 were prepared from the reaction of 1,4,8,11-tetraazatricyclo[9.3.1.1^{4,8}]hexadecane with two equivalents of 3-chloromethyl-5-methyl salicylaldehyde and 3-chloromethyl-5-bromo salicylaldehyde, respectively. PC-1 and PC-2 were hydrolyzed with NaOH to yield the macrocyclic ligands L^1 and L^3, respectively. The macrocyclic ligands L^2 and L^4 were prepared by the reduction of PC-1 and PC-2 with excess $NaBH_4$ in ethanol. The mononuclear copper(II) and nickel(II) complexes were prepared from an equimolar amount of ligand and corresponding metal(II) perchlorate. The synthetic routes for ligands and complexes are shown in schemes 1 and 2, respectively. The complexes were characterized by spectral studies, magnetic, electrochemical and catalytic behavior. Crystals of L^1 of X-ray quality were obtained from chloroform by slow evaporation at room temperature [20].

3.1. *Spectral studies*

The IR spectra of L^1–L^4 show a sharp band at 1680 cm^{-1} due to the presence of CHO group. Bands around 3290 cm^{-1} are indicative of νN–H in the ligands. The OH group in all the ligands show a peak at 3400 cm^{-1}. Due to tetra substitution, νN–H peaks are absent in L^2 and L^4. All the complexes show a sharp band at 1665–1678 cm^{-1} due to νC=O stretching, indicating the carbonyl is not coordinated to the metal. Uncoordinated perchlorate anions in all complexes are inferred from single broad bands around 1100 cm^{-1} (ν_3-antisymmetric stretching) which are not split and a band around 650 cm^{-1} (ν_4-antisymmetric bending). The band around 930 cm^{-1} (ν_2-symmetric stretching) due to coordinated perchlorate is not observed [21, 22]. All the complexes show a peak around 3400 cm^{-1}, showing that OH is not coordinated with the metal.

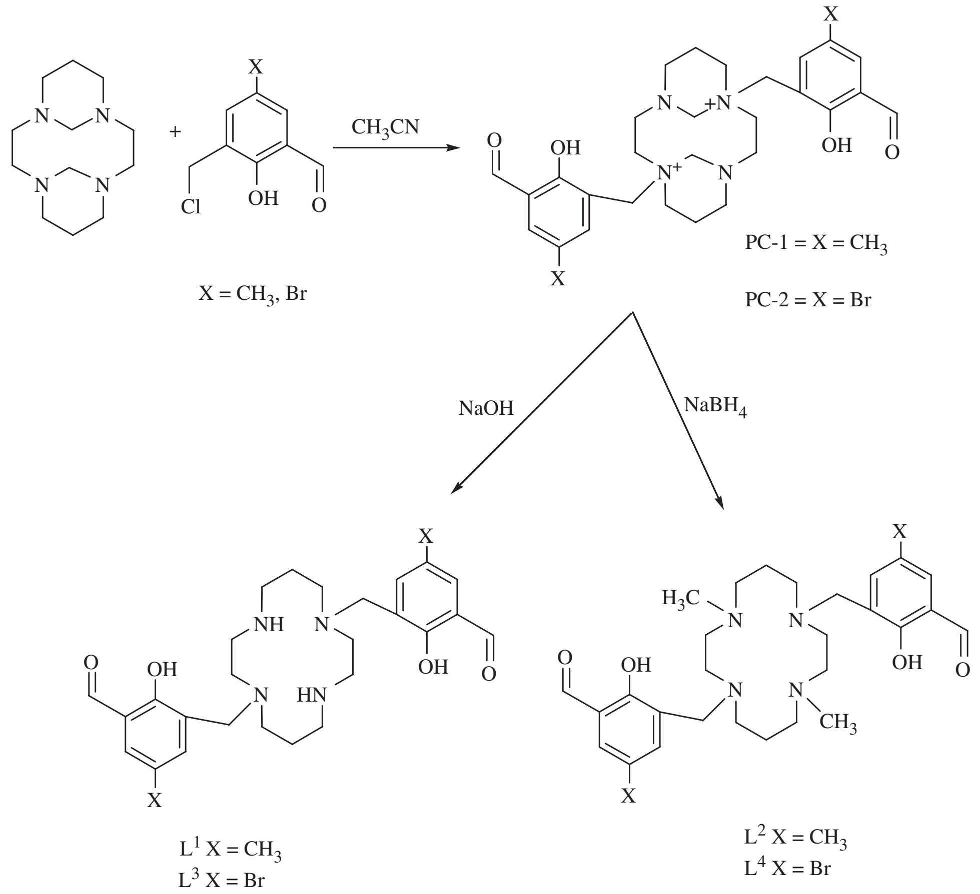

Scheme 1. Synthesis of N-substituted ligands.

The electronic spectra of all the complexes exhibit three main features: (i) one or two peaks in the range of 250–300 nm assigned to the intra-ligand charge transfer transition (π–π^*), (ii) an intense peak in the range of 380–400 nm is due to ligand-to-metal charge transfer, and (iii) all the copper(II) complexes show d-d transitions in the region of 500–555 nm, typical for square planar tetraazamacrocyclic copper(II) complexes [23, 24]. The electronic spectra of nickel(II) complexes show d–d bands in the region 480–500 nm, consistent with square planar geometry with N_4 coordination [25, 26a]. The observed d-d bands for unsubstituted copper(II) and nickel(II) macrocyclic complexes are 450 and 517 nm, respectively [47]. The electronic spectra of the complexes show a red shift on increasing N-alkylation. The electronic spectra values are given in table 1. The red shift in the d-d absorption bands of the copper(II) and nickel(II) complexes may be due to tetrahedral distortion of the coordination sphere caused by N-alkylation [26b].

The ^{1}H NMR spectra of the ligands show a singlet in the range of δ 12.30–12.60 ppm for phenolic OH protons and the aromatic aldehyde is singlet in the range of δ 9.98–10.20 ppm. The nickel(II) complexes show a singlet at δ 13.40 ppm due to phenolic proton and a singlet at δ 10.30 ppm due to aldehyde proton. This shows that

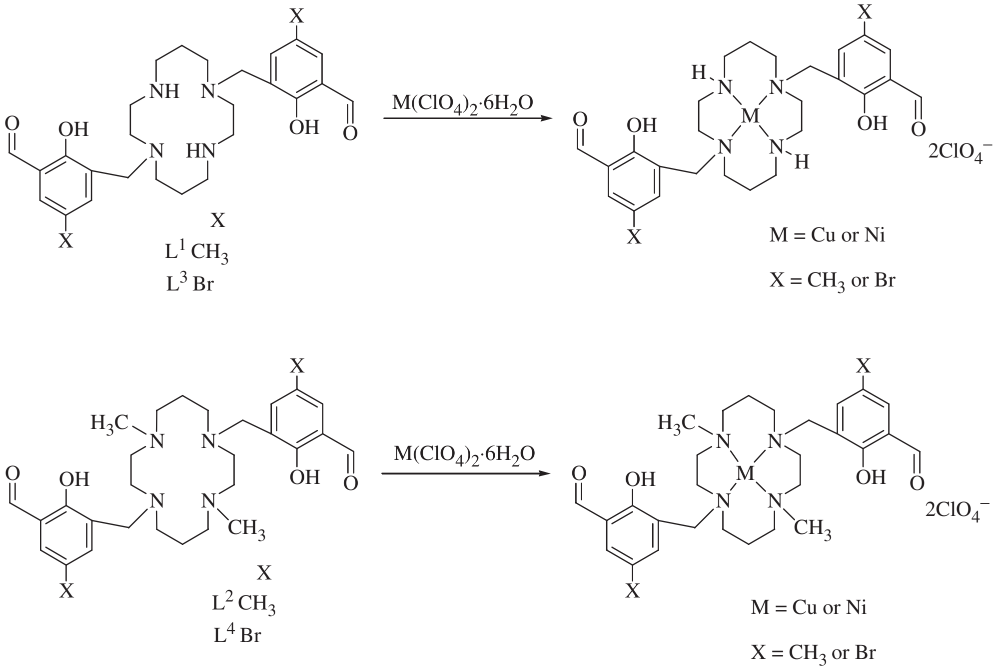

Scheme 2. Synthesis of mononuclear copper(II) and nickel(II) complexes.

Table 1. Electronic, magnetic and ESR spectral data of the complexes.

Compound	[(λ_{max} (nm)) (ε, M^{-1} cm^{-1})] in CH$_3$CN	Magnetic moment μ_{eff} BM	ESR		
			$g_{\parallel}$	$g_{\perp}$	$A_{\parallel}$
L^1	281 (22,450), 258 (26,400)				
L^2	294 (20,640), 261 (24,540)				
L^3	289 (22,760), 262 (24,480)				
L^4	296 (21,440), 268 (25,760)				
[CuL^1](ClO$_4$)$_2$	512 (169) 394 (15,400), 302 (33,600)	1.72	2.31	2.09	160
[CuL^2](ClO$_4$)$_2$	554 (181) 392 (11,600), 311 (32,408)	1.72	2.21	2.05	165
[CuL^3](ClO$_4$)$_2$	518 (172) 378 (12,934), 303 (29,187)	1.74	2.18	2.10	172
[CuL^4](ClO$_4$)$_2$	560 (179) 389 (12,642), 305 (32,342)	1.72	2.31	2.06	175
[NiL^1](ClO$_4$)$_2$	478 (186) 376 (11,421), 300 (30, 347)				
[NiL^2](ClO$_4$)$_2$	491 (164) 385 (12,524), 300 (30, 320)				
[NiL^3](ClO$_4$)$_2$	482 (182) 371 (12,243), 301 (31, 434)				
[NiL^4](ClO$_4$)$_2$	497 (180) 383 (13,548), 305 (32, 212)				

the phenolic OH group and the aromatic aldehyde are not coordinated to the metal. Figure 1 shows the ^{1}H NMR spectrum of [NiL^1](ClO$_4$)$_2$.

3.2. *Magnetic properties of the complexes*

All the copper complexes show four lines in the ESR spectrum with nuclear hyperfine spin 3/2. The hyperfine $A_{\parallel}$ splitting falls in the range of 150–160 × 10^{-4} cm^{-1}, indicative

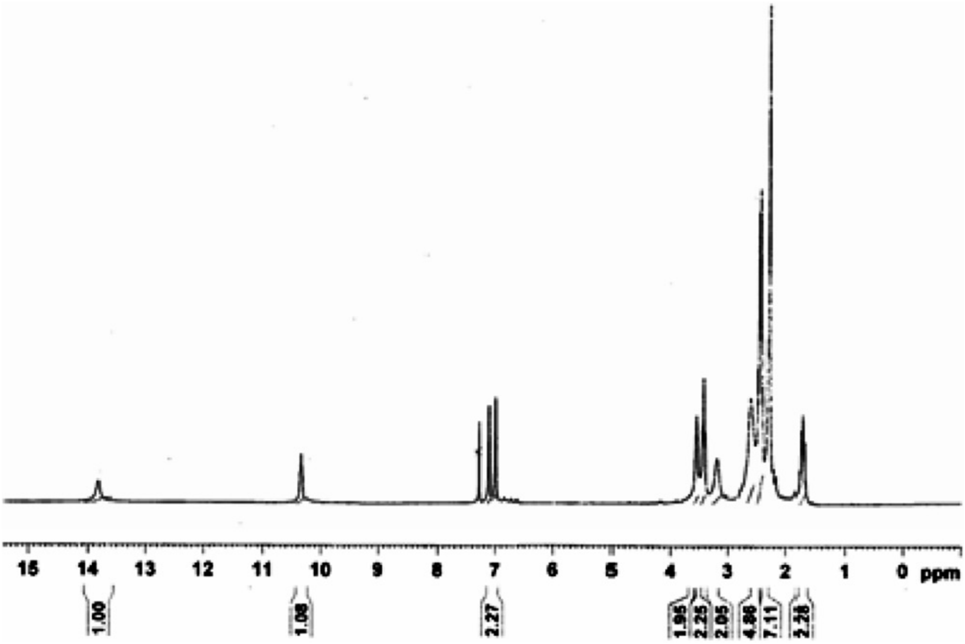

Figure 1. ^{1}H NMR spectrum of $[NiL^1](ClO_4)_2$.

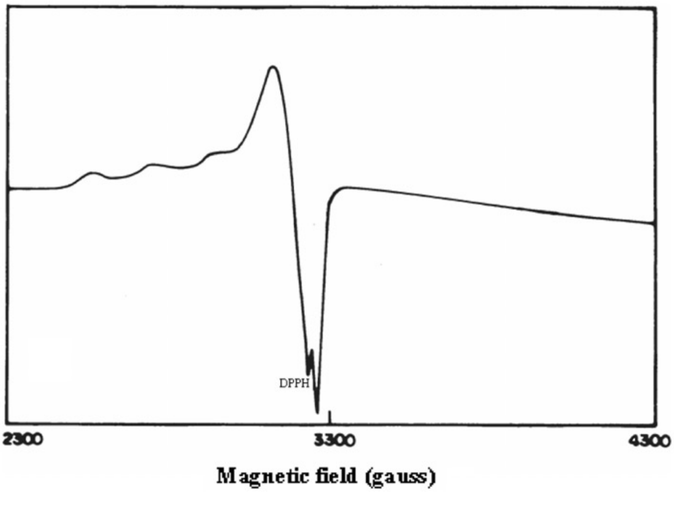

Figure 2. ESR spectrum of $[CuL^1](ClO_4)_2$.

of an electron interacting with only one copper nucleus. The relation $g_{\|} > g_{\perp}$ is typical of d^9 copper(II) complexes in a ground state doublet with the unpaired electron in a $d_{x^2-y^2}$ orbital [27, 28]. The g and $A_{\|}$ values of (CuL^1–CuL^4) are close to the $[Cu(cyclam)]^{2+}$ suggesting essentially square-planar coordination geometry of the mononuclear copper(II) complexes [29–33]. Figure 2 shows the ESR spectrum of $[CuL^1](ClO_4)_2$. The ESR spectrum values of all the copper(II) complexes are given in table 1.

Table 2. Electrochemical data* for the complexes (reduction at cathodic potential).

No.	Complexes	E_{Pc} (V)	E_{Pa} (V)	$E_{1/2}$ (V)	ΔE (mV)
1	$[CuL^1](ClO_4)_2$	−1	−0.84	−0.92	160
2	$[CuL^2](ClO_4)_2$	−0.96	−0.78	−0.87	120
3	$[CuL^3](ClO_4)_2$	−1.04	−0.92	−0.98	120
4	$[CuL^4](ClO_4)_2$	−0.94	−0.8	−0.87	140
5	$[NiL^1](ClO_4)_2$	−1.3	−0.98	−1.14	360
6	$[NiL^2](ClO_4)_2$	−1.18	−0.84	−1.01	340
7	$[NiL^3](ClO_4)_2$	−1.26	−0.94	−1.1	320
8	$[NiL^4](ClO_4)_2$	−1.21	−0.88	−1.04	320

*Measured by CV at $50\,mV\,s^{-1}$. E *vs.* Ag/AgCl conditions: GC working and Ag/AgCl reference electrodes; supporting electrolyte TBAP; concentration of complex 1×10^{-3} M, concentration of TBAP 1×10^{-1} M.

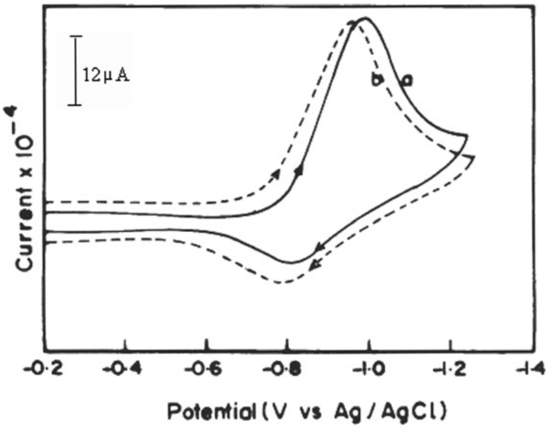

Figure 3. Cyclic voltammogram of (a) $[CuL^1](ClO_4)_2$; (b) $[CuL^2](ClO_4)_2$ (reduction process).

The room temperature (at 298 K) magnetic moment studies of copper(II) complexes show a μ_{eff} in the range of 1.70–1.74 BM, close to the spin-only value of copper(II) [18]. The magnetic moment values of the copper(II) complexes are given in table 1. The nickel(II) complexes are diamagnetic due to square planar geometry around the metal [34].

3.3. *Electrochemical properties of the complexes*

The molar conductance values of the complexes in dimethylformamide fall in the range of 133–159 $\Lambda_m/S\,cm^{-1}\,mol^{-1}$, indicating 1 : 2 electrolytes [35]. The electrochemical data are summarized in table 2. The cyclic voltammograms for the copper(II) complexes are shown in figure 3 and for nickel(II) complexes shown in figure 4.

3.4. *Reduction process at negative potential*

The cyclic voltammogram of the copper(II) and nickel(II) complexes were recorded in the potential range 0 to −1.4 V. Cyclic voltammograms for copper(II) complexes are

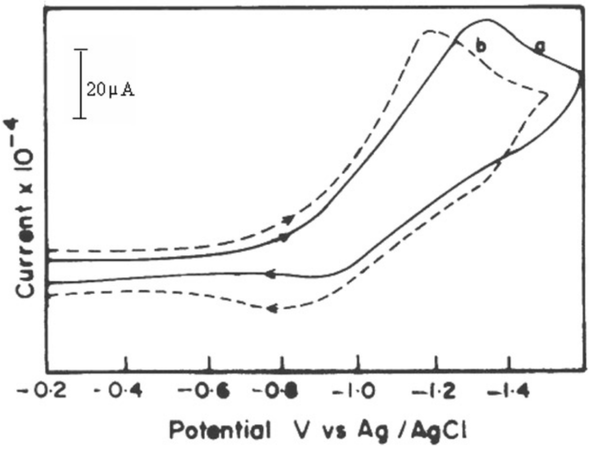

Figure 4. Cyclic voltammogram of (a) $[NiL^1](ClO_4)_2$; (b) $[NiL^2](ClO_4)_2$ (reduction process).

shown in figure 3. Each voltammogram shows one quasireversible reduction wave [36] at negative potential (−0.94 to −1.04 V). The reduction processes are quasireversible, as evident from the following criteria: ΔE increases with increasing scan rate and is always greater than 60 mV. Controlled potential electrolysis carried out at 100 mV more negative than the reduction wave consumes one electron per molecule.

The reduction potentials of the copper complexes shift anodically from the L^1 ($E_{pc} = -1.00$) V to L^2 ($E_{pc} = -0.94$) V, due to (i) the steric effect of the methyl groups on two *trans*-nitrogens of the macrocycle, causing distortion of the geometry of the complexes (due to macrocyclic distortion). (ii) The increase in tertiary nitrogens in L^2 causes more distortion of the coordination geometry around the metal ion making the system more flexible, which stabilizes Cu(I) [37–42]. The one electron process occurred at the electrode surface was inferred to be

$$\mathbf{Cu^{II}} \rightleftharpoons \mathbf{Cu^{I}}$$

The same trend was observed for nickel(II) complexes, where N-alkylation of the macrocyclic framework stabilizes the monovalent metal ions by increasing the cavity size of the macrocyclic ligand and decreasing the ligand field strength imparted by the nitrogen donor [43]. The copper(II) and nickel(II) complexes of the ligands L^3 and L^4 also show the same type of cyclic voltammograms with slight variation in the reduction potential.

3.5. *Oxidation process at positive potential*

The cyclic voltammograms for nickel(II) complexes were recorded at anodic potential in the range 0 to +1.6 V. Each voltammogram shows one quasireversible oxidation wave [36] at a positive potential (+1.24 to +1.38 V), shown in figure 5. The electrochemical data are summarized in table 3. Controlled potential electrolysis indicates consumption of one electron per molecule. The oxidation potentials of nickel(II) complexes shift towards positive potential [36] as the number of tertiary nitrogens increase. Since L^2

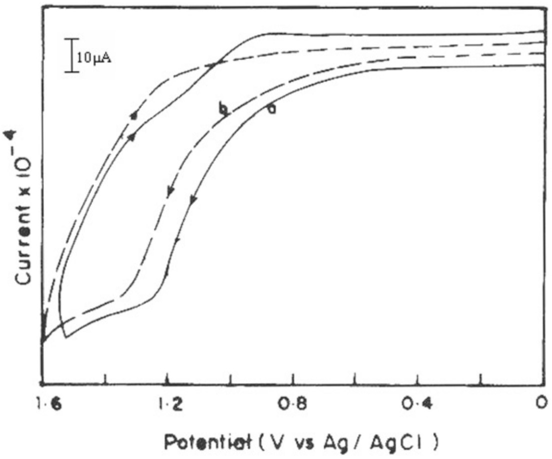

Figure 5. Cyclic voltammogram of (a) $[NiL^1](ClO_4)_2$; (b) $[NiL^2](ClO_4)_2$ (oxidation process).

Table 3. Electrochemical data* for the complexes (oxidation at anodic potential).

No.	Complexes	E_{Pc} (V)	E_{Pa} (V)	$E_{1/2}$ (V)	ΔE (mV)
1	$[NiL^1](ClO_4)_2$	1.24	0.98	1.08	260
2	$[NiL^2](ClO_4)_2$	1.34	1.2	1.27	140
3	$[NiL^3](ClO_4)_2$	1.26	1.11	1.18	150
4	$[NiL^4](ClO_4)_2$	1.38	1.23	1.3	150

*Measured by CV at 50 mV s^{-1}. E *vs.* Ag/AgCl conditions: GC working and Ag/AgCl reference electrodes; supporting electrolyte TBAP; concentration of complex 1×10^{-3} M, concentration of TBAP 1×10^{-1} M.

stabilizes the lower oxidation state, oxidation of $[NiL^2ClO_4)_2]$ is more difficult than $[NiL^1(ClO_4)_2]$. The same trend was also observed for nickel(II) complexes of L^3 and L^4.

$$Ni^{II} \rightleftharpoons Ni^{III}$$

The present study and literature reports establish that a decrease in the ligand field strength of the macrocyclic ligand results in an anodic shift of the reduction potentials of their metal complexes [36]. Alternatively the anodic shift in the reduction potential of the copper(II) and nickel(II) complexes could be attributed to tetrahedral distortion of the coordination sphere caused by steric strain induced by the N-alkylation [26b].

3.6. *Kinetic studies*

3.6.1. Oxidation of pyrocatechol (catecholase activity). The catecholase activity of the copper(II) complexes was carried out using pyrocatechol as the model substrate for identification of functional models for metalloenzymes [44, 45]. Solutions (10^{-3} mol dm^{-3}) of complexes in dimethylformamide were treated with 100 equivalents of pyrocatechol in the presence of air. The reaction was followed every 5 min spectrophotometrically at 390 nm for 45 min. The slope was determined from initial

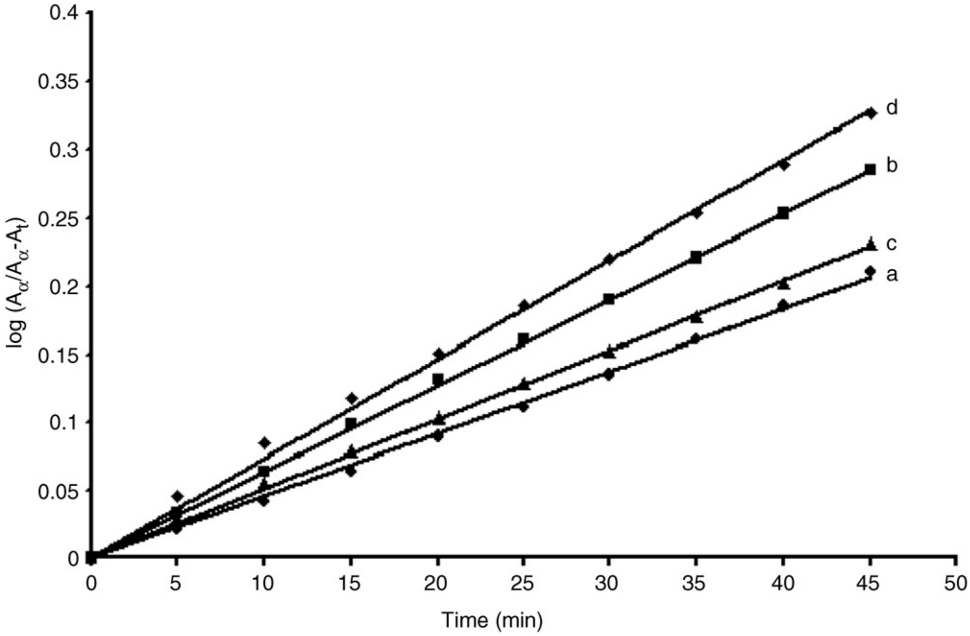

Figure 6. Catecholase activity of (a) $[CuL^1](ClO_4)_2$; (b) $[CuL^2](ClO_4)_2$; (c) $[CuL^3](ClO_4)_2$; (d) $[CuL^4](ClO_4)_2$.

Table 4. Hydrolysis of 4-nitrophenyl phosphate* and catecholase activity*.

		Rate constant (k) $(\times 10^{-3})\,\mathrm{min}^{-1}$	
No.	Complexes	Catecholase	NPP
1	$CuL^1(ClO_4)_2$	11.2	13.5
2	$CuL^2(ClO_4)_2$	13.5	17.9
3	$CuL^3(ClO_4)_2$	12.6	11.9
4	$CuL^4(ClO_4)_2$	15.9	19.2
5	$NiL^1(ClO_4)_2$	–	12.5
6	$NiL^2(ClO_4)_2$	–	19.4
7	$NiL^3(ClO_4)_2$	–	16.8
8	$NiL^4(ClO_4)_2$	–	21

*Measured spectrophotometrically in DMF.
Concentration of the complexes: 1×10^{-3} M.
Concentration of 4-nitrophenylphosphate: 1×10^{-1} M.
Concentration of pyrocatechol: 1×10^{-1} M.

rates by monitoring the growth of the 390 nm band of the o-quinone product. A linear relationship for initial rate and the complex concentration obtained for the copper(II) complexes shows first-order dependence on the complex concentration.

Plots of log $(A_\alpha/A_\alpha - A_t)$ *versus* time for catecholase activity of the copper(II) complexes are shown in figure 6. The observed initial rate constants are given in table 4. $[CuL^2](ClO_4)_2$ has higher catalytic activity ($13.5 \times 10^{-3}\,\mathrm{min}^{-1}$) than $[CuL^1](ClO_4)_2$ ($11.2 \times 110^{-3}\,\mathrm{min}^{-1}$). The rate of oxidation of catechol to o-quinone increases as the macrocyclic N-alkylation increases [29, 46], perhaps due to flexibility resulting from

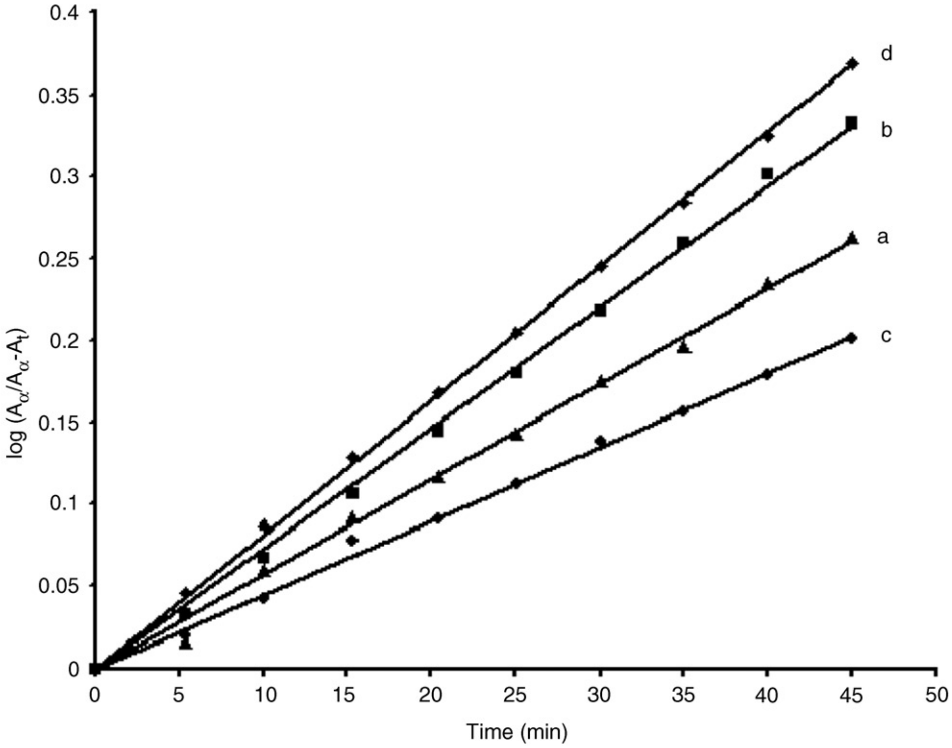

Figure 7. Hydrolysis of 4-nitrophenylphosphate by (a) $[CuL^1](ClO_4)_2$; (b) $[CuL^2](ClO_4)_2$; (c) $[NiL^1](ClO_4)_2$; (d) $[NiL^2](ClO_4)_2$.

distortion of the coordination sphere on N-alkylation. This geometry may favor substrate coordination in the axial position, which in turn increases the rate of reaction [47].

3.6.2. Kinetic studies of hydrolysis of 4-nitrophenylphosphate. The catalytic activity of the copper(II) and nickel(II) complexes on hydrolysis of 4-nitrophenylphosphate was determined spectrophotometrically by monitoring the increase in the characteristic absorbance of the 4-nitrophenolate anion at 420 nm in dimethylformamide at 25°C. For this purpose, 10^{-3} mol dm^{-3} solutions of complexes were treated with 100 equivalents of 4-nitrophenyl phosphate in the presence of air.

The course of the reaction was followed at 420 nm for 45 min at regular time intervals. The slope was determined by the method of initial rates by monitoring the growth of 4-nitrophenolate anion. A linear relationship for all the complexes shows a first-order dependence on the complex concentration. Plots of log $(A_\alpha/A_\alpha - A_t)$ *versus* time for hydrolysis of 4-nitrophenylphosphate are shown in figure 7. The observed initial rate constants for the copper(II) and nickel(II) complexes are given in table 4. The rates of hydrolysis catalyzed by the complexes of L^2 and L^4 were higher than those of L^1 and L^3 i.e. the catalytic activity of copper(II) and nickel(II) complexes increases on N-alkylation.

The higher activity of [NiL^2(ClO$_4$)$_2$] is $19.40 \times 10^{-3}\,\mathrm{min}^{-1}$ than [NiL^1(ClO$_4$)$_2$] (12.4×10^{-3}) may be due to greater distortion of the geometry of the complex with N-alkylation [48]. This distortion in geometry is inferred from the absorption spectra of the complexes. The di N-substituted nickel(II) complex has d-d bands at 478 and 482 nm, and for tetra N-substituted macrocycle at 491 and 497 nm, respectively. The di N-substituted copper(II) complex has d-d bands at 512 and 518 nm, tetra N-substituted copper complex at 554 and 560 nm, respectively [48]. This red shift in the wavelength indicates that the coordination in the tetra N-substituted complex is more distorted than that of the di N-substituted complex [49]. It is evident from the literature [50], the rate constant for more distorted complex is higher than for less-distorted complex. On comparison of the hydrolysis of 4-nitrophenylphosphate by nickel(II) and copper(II) complexes, the nickel(II) complexes have higher rate constants than the copper complexes, similar to nickel(II) (tren) complexes reported by De Rosch and Trogler [47].

4. Summary

N-substituted cyclam-based copper(II) and nickel(II) complexes have been prepared and characterized. The complexes show significant change in their characteristics by increasing N-alkylation, (a) a red shift observed in the electronic spectra of the complexes, (b) anodic shifts in the reduction potential of the complexes and (c) increasing catalytic activity of the complexes. The effect of N-alkylation on the reduction potential and the red shift in the d-d absorption bands of the complexes could in principle be attributed to a tetrahedral distortion of the coordination geometry due to steric strain.

Acknowledgements

Financial support from the University Grants Commission (RGNF), New Delhi, is gratefully acknowledged.

References

[1] V. Alexander. *Chem. Rev.*, **95**, 273 (1995).
[2] P. Caravan, J.J. Ellison, T.J. McMurry, R.B. Laufter. *Chem. Rev.*, **99**, 2293 (1999).
[3] L.F. Lindoy. *The Chemistry of Macrocyclic Ligand Complexes*, Cambridge University Press, Cambridge (1989).
[4] A. Bianchi, L. Calabi, F. Corana, S. Fontana, P. Losi, A. Maiocchi, L. Paleari, B. Valtancoli. *Coord. Chem. Rev.*, **204**, 309 (2000).
[5] O. Reany, T. Gunnlaugsson, D. Parker. *Chem. Commun.*, 473 (2000).
[6] D.M. Epstein, L.L. Chappell, H. Khalili, R.M. Supkows, W.D. Horrocks, J.R. Morrow. *Inorg. Chem.*, **39**, 2130 (2000).
[7] M.W. Brechbiel, C.G. Pippin, T.J. McMurry, D. Milenic, M. Roselli, D. Colcher, O.A. Gansow. *J. Chem. Soc., Chem. Commun.*, 1169 (1991).
[8] H. Fensterbank, J. Zhu, D. Riou, C. Larpent. *J. Chem. Soc., Perkin Trans.*, **1**, 811 (1999).
[9] A.K. Mishra, K. Draillard, A. Faivre-Chauvet, J.F. Gestin, C. Curtet, J.F. Chatal. *Tetrahedron Lett.*, **37**, 7515 (1996).

[10] (a) J. Chappman, G. Ferguson, J.F. Gallagher, M.C. Jennings, D. Parker. *J. Chem. Soc. Dalton Trans.*, 345 (1992); (b) S.G. Kang, M.S Kim, J.S. Choi, D. Whang, K. Kim. *J. Chem. Soc., Dalton Trans.*, 363 (1995).

[11] C. Gerdemann, C. Eicken, B. Kerbs. *Acc. Chem. Res.*, **35**, 183 (2002).

[12] E.I. Solomon, P. Chen, M. Metz, S.K. Lee, A.E. Palmer. *Angew. Chem. Int. Ed.*, **40**, 4570 (2001).

[13] G.J. Kiny, B. Zemer. *Inorg. Chim. Acta*, **225**, 381 (1997).

[14] J. Kwakami, Y. Komai, T. Sumori, A. Fukushi, K. Shimozaki, S. Ito. *J. Photochem. Photobiol A: Chem.*, **139**, 71 (2001).

[15] H. Yamamoto, A. Ori, K. Ueda, C. Dusemund, S. Shinkai. *Chem. Commun.*, 407 (1996).

[16] E.K. Barrefield, F. Wagner. *Inorg. Synth.*, **16**, 220 (1976).

[17] J.C. Duff. *J. Chem. Soc.*, 547 (1941).

[18] J.D. Gane, D.E. Fenton, J.M. Latour, A.J. Smith. *J. Chem. Soc., Dalton Trans.*, 2279 (1991).

[19] G. Royal, V.D. Gindrey, S. Dahaowi, A. Tabard, R. Guilard, P. Pullumbi, C. Lecomte. *Eur. J. Org. Chem.*, 1971 (1998).

[20] D. Gayathri, D. Velmurugan, K. Ravikumar, S. Sreedaran, V. Narayanan. *Acta Cryst.*, **E62**, o3714 (2006).

[21] K. Nakamoto. *Infrared and Raman Spectra of Inorganic and Coordination Compounds*, Wiley-Interscience, New York (1978).

[22] B.J. Hathaway, A.E. Underhill. *J. Chem. Soc.*, 3091 (1961).

[23] (a) D. Meyerstein. *Coord. Chem. Rev.*, **185**, 141 (1999); (b) R. Buxtrof, T.A. Kaden. *Helv. Chim. Acta*, **57**, 1035 (1974); (c) M. Heidger, T.A. Kaden. *Helv. Chim. Acta*, **66**, 86 (1983).

[24] (a) L. Fabbrizzi, L. Montanga, A. Poggi, T.A. Kaden, L.C. Siegfried. *J. Chem. Soc. Dalton Trans.*, 2631 (1987); (b) J. Chapman, G. Ferguson, J.F. Gallagher, M.C. Jennings, D. Parker. *J. Chem. Soc. Dalton Trans.*, 345 (1992).

[25] S.J. Brudenell, L. Spiccia, A.M. Bond, P.C. Mahon, D.C.R. Hockless. *J. Chem. Soc. Dalton Trans.*, 3919 (1998).

[26] (a) A.B.P. Lever. *Inorganic Electronic Spectroscopy*, 2nd Edn, Elsevier, Amsterdam (1984); (b) G. Golub, H. Cohen, P. Paoletti, A. Bencini, L. Messori, I. Bertini, D. Meyerstein. *J. Am. Chem. Soc.*, **117**, 8353 (1995).

[27] S. Zhu, F. Kon, H. Lin, E. Lin. *Inorg. Chem.*, **35**, 3848 (1996).

[28] R.C. Agarwal, N.K. Singh, R.P. Singh. *Inorg. Chem.*, **20**, 2794 (1981).

[29] H. Kurosaki, C. Bucher, E. Espinosa, J.M. Barbe, G. Guilard. *Inorg. Chim. Acta*, **322**, 145 (2001).

[30] J. Gradinaru, A. Forni, Y. Simonov, M. Popovici, S. Zecchin, M. Gdaniec, D.E. Fenton. *Inorg. Chim. Acta*, **357**, 2728 (2004).

[31] S.V. Rasokha, Y.D. Lampeka, I.M. Maloshtan. *J. Chem. Soc. Dalton Trans.*, 631 (1993).

[32] M. Lachkar, G. Guilard, A. Atmani, A. De Cian, J. Fisher, R. Weiss. *Inorg. Chem.*, **37**, 1575 (1998).

[33] E. Zeigerson, G. Ginzburg, D. Meyerstein, L.J. Kirschenbaum. *J. Chem. Soc. Dalton Trans.*, 1243 (1980).

[34] (a) A. Bottcher, H. Elias, E. Jager, H. Langfelderova, M. Mazur, L. Mullor, H. Paulus, P. Pelikan, M. Rudolph, M. Valko. *Inorg. Chem.*, **32**, 4131 (1993).

[35] J. Geary. *Coord. Chem. Rev.*, **7**, 81 (1971).

[36] (a) H. Okawa, M. Tadokora, T.Y. Aretake, M. Ohba, K. Shindo, M. Mitsumi, M. Koikawa, M. Tomono, D.E. Fenton. *J. Chem. Soc. Dalton Trans.*, 253 (1993); (b) E.K. Barefield, G.M. Freeman, D.G. Van Derveer. *Inorg. Chem.*, **25**, 552 (1986).

[37] P.V. Bernhart, J.M. Harrowfield, D.C.R. Hockless, A.M. Sargeson. *Inorg. Chem.*, **33**, 5659 (1994).

[38] G. Golub, H. Cohen, P. Paoletti, A. Bencini, L. Messori, I. Bertini, D. Meyerstein. *J. Am. Chem. Soc.*, **117**, 8553 (1995).

[39] J. Manonmani, M. Thirumurugan, M. Kandaswamy, V. Narayanan, S. Shanmuga Sundararaj, M.N. Ponnuswamy, G. Shanmugam, H.K. Fun. *Polyhedron*, **20**, 3039 (2001).

[40] E. Gao, W. Bu, G. Yang, D. Liao, Z. Jiang, S. Yan, G. Wang. *J. Chem. Soc. Dalton Trans.*, 1431 (2000).

[41] (a) P.A. Connick, K.A. Macor. *Inorg. Chem.*, **30**, 4654 (1991); (b) N. Sengottuvelan, D. Saravanakumar, M. Kandaswamy. *Inorg. Chim. Acta*, **8**, 297 (2005).

[42] E. Monzani, L. Quinti, A. Perotti, L. Casella, G. Tabbi, P. Faleschini, L. Randaccio, S. Geremia, G. Nardin. *Inorg. Chem.*, **37**, 553 (1998).

[43] (a) C. Belle, C. Beguin, I. Gautier-Luneau, S. Hamman, C. Philouze, J.L. Pierre, F. Thomas, S. Torelli. *Inorg. Chem.*, **41**, 479 (2002); (b) P.V. Bernhardt, J.M. Harrowfield, D.C.R. Hockless, A.M. Sargeson. *Inorg. Chem.*, **33**, 5659 (1994).

[44] K. Moore, G.S. Vigee. *Inorg. Chim. Acta*, **66**, 125 (1982).

[45] D. Bolus, G.S. Vigee. *Inorg. Chim. Acta*, **67**, 19 (1982).

[46] W.A. Nathaniel, P. Moore, K.F. Mok. *J. Chem. Soc. Perkin Trans.*, **2**, 1186 (1980).

[47] M.D. De Rosch, W.C. Trogler. *Inorg. Chem.*, **29**, 2409 (1990).

[48] J.R. Roper, H. Elias. *Inorg. Chem.*, **31**, 1202 (1992).

[49] M. Jaacobi, D. Meyerstein, J. Lilie. *Inorg. Chem.*, **18**, 429 (1979).

[50] R. Bhalla, M. Helliwell, C.D. Garner. *Inorg. Chem.*, **36**, 2944 (1997).